Thermochimica Acta 495 (2009) 57–62

Contents lists available at ScienceDirect

Thermochimica Acta

journal homepage: www.elsevier.com/locate/tca

Study on the morphology, crystalline structure and thermal properties of yellow ginger starch acetates with different degrees of substitution

Liming Zhang[a,*], Weiguang Xie[a], Xi Zhao[c], Ying Liu[b], Wenyuan Gao[c]

[a] Key Laboratory of Industrial Microbiology, Ministry of Education, Tianjin University of Science and Technology, Tianjin 300457, China
[b] College of Bioengineering, Tianjin University of Science and Technology, Tianjin 300457, China
[c] School of Pharmaceutical Science and Technology, Tianjin University, Tianjin 30072, China

ARTICLE INFO

Article history:
Received 15 January 2009
Received in revised form 25 May 2009
Accepted 29 May 2009
Available online 12 June 2009

Keywords:
Yellow ginger
Starch acetate
Degrees of substitution
Physicochemical properties

ABSTRACT

Yellow ginger starch acetates with different degrees of substitution (DS) were prepared by reacting native starch with glacial acetic acid/acetic anhydride using sulfuric acid as catalyst. X-ray diffraction (XRD) of acetylated starch revealed that the crystal structure of native starch was disappeared and new crystalline regions were formed. Their formation was confirmed by the presence of the carbonyl signal around 1750 cm^{-1}, as well as the reduced hydroxyl groups, in the Fourier transform infrared spectroscopy (FT-IR). The scanning electron microscopy (SEM) suggested most of the starch granules disintegrated with many visible fragments along with the increasing DS. The thermal behavior of the native starch and starch acetate were investigated using thermogravimetric analysis (TGA) and differential thermal analysis (DTA), it was observed that the thermal stability of acetylated starch depends on the degree of substitution. Thermal stability of high DS acetylated starch is much better than that of the original starch when DS reached to 2.67.

1. Introduction

Yellow ginger, whose scientific name is *Dioscorea zingiberensis* C.H. Wright, is a perennial grass vine plant. With its rootstocks containing rich saponins, it is a starting raw material for steroid medicine and is widely applied in medicines for contraception, analgesia and anesthesia, etc. [1]. Yellow ginger is unique to China and it is mainly distributed from the upper reaches of Hanjiang Basin of Wudang Mountain in Hubei province to the northern foot of the Qinling Mountains in Shanxi province. Currently, over 10 provinces and cities in China have developed the yellow ginger industry. The area of yellow ginger bases has been developed to over 166,750 ha, the number of saponins processing enterprises has reached nearly 200 and the production capacity of saponins has reached over 5000 t [2]. In the rhizome of fresh yellow ginger cultivars, starch is the main components making up 13–18% content in the total biomass [3].

The traditional processing technique wastes a large amount of resources. Starch and cellulose are discarded and become the main contents in the water pollutants. The large amount of waste water discharged during yellow ginger processing contained strong acid and the input of treatment is quite high. As for an enterprise with an annual output of 100 t saponins, it will need about Renminbi (RMB) 5–8 million yuan for the disposal work [4]. Therefore, cleaner production is an inevitable choice for extracting saponins from yellow ginger. The ideas of circular economy and cleaner production are consistently implemented in the technique development and application. Under the prerequisite of guaranteeing the saponin recovery rate, physical methods are adopted to separate the starch and cellulose in yellow ginger in order to realize the utilization of wastes as resources and improve economic benefits.

It is well known that extensive research has been conducted on the structure and functional properties of the commercial starches obtained from crops due to their ready availability and their extensive utilization in food and non-food applications [5]. However, the starch derived from medicinal plants has not been paid enough attention by starch researchers. In order to widen the application of these plants which contained plenty of starches and provide a new starch for the food and pharmaceutical industry, the effort should have been made to investigate the physicochemical properties of these starches and their modification.

Native starch has the disadvantages of hydrophilicity, poor mechanical properties and dimensional stability, especially in presence of water and in humid environments [6]. Starch modification can overcome these shortcomings by means of altering the structure and affecting the hydrogen bonding of amylose and amylopectin in a controllable manner to enhance and extend starch application. Following crosslinking, esterification and etherification are the second important modifications in the starch industry [7]. The most typical starch ester is acetylated starch, which is

* Corresponding author. Tel.: +86 22 60601265.
E-mail address: zhanglmd@yahoo.com.cn (L. Zhang).

0040-6031/$ – see front matter © 2009 Elsevier B.V. All rights reserved.
doi:10.1016/j.tca.2009.05.019

actively marketed due to the specific properties arising from the substitution groups. The introduction of acetyl groups interrupts the ordered structure of native starch and interferes with the re-association of amylose and amylopectin in gelatinized starch, leading to the change in morphological properties, crystalline properties, gelatinization properties involving transition temperatures and gelatinization enthalpy of the starch [8]. Starches with DS of 0.01–0.2 are of commercial interest because of their usage based on properties with respect to film forming, binding, adhesion, thickening, stabilizing and texturing. Highly acetylated starch with a degree of substitution (DS) of 2–3 was of research interest from 1950 through 1980 for their solubility into acetone and chloroform and for their thermo plasticity [9]. As a biodegradable carbohydrate polymer material, acetylated starch also has many potential uses in pharmaceutical applications [10]. Therefore, acetylated starch could have potential use in food and pharmaceutical industries.

The purpose of this study was to understand the changes of yellow ginger starch before and after esterification. The morphology and crystalline structure of yellow ginger acetates with different degrees of substitution were investigated by IR, SEM and XRD. The materials were then treated to thermal analysis, using TG–DTG and DTA to examine whether esterification had any effect on the thermal behavior of starch granules. With the obtained result, it is possible to precisely evaluate the availability and provide sufficient parameters to all kinds of uses of yellow ginger starch.

2. Materials and methods

2.1. Materials

The yellow ginger (*D. zingiberensis* C.H. Wright) tubers were provided by Ankang medicine Co., Shanxi, China (November, 2007). These tubers were cultivated (under soil conditions) in the province of Shanxi, China for 2 years cultivation period.

2.2. Starch extraction

In the yellow ginger starch isolation, the tubers were trimmed to get rid of defective parts and washed with water, and then the tubers were sliced into pieces with the thickness between 3 and 5 mm and dried in an oven until weight constancy. The small slices were incubated in 0.2% (w/v) NaOH solution (pH 10–11) for 24 h, in order to macerate the botanical cell wall and to reduce activities of microbes and enzymes that may decompose starches. After the tubers were milled, the slurry was filtered through 150 μm screen. The supernatant was milled for several times and the slurry refiltered through 150 μm screen to keep the cell wall off the starch slurry. Then the residue was amassed and deposited quietly for 6 h. The liquid layer was discarded and the superficial impurity of starch was eradicated. Ethanol (95%) was added to remove the scanty dioscin. Subsequently, the starch fraction was raised several times with distilled water until a neutral pH was reached. The slurry was sieved with 75 μm mesh size several times. The starch suspension obtained was dried in a convection oven at 50 °C until weight constancy. The dried material was milled and sieved with 75 μm screen to get the starch flour [11]. Zhou et al. [12] and Wang et al. [13] have examined the yellow ginger starch for its chemical composition, amylose content and physicochemical properties in paper.

2.3. Preparation of starch acetates

The dry native starch of 10.0 g was stirred with 10.0 mL glacial acetic acid at room temperature for about 2 min. Then 30.0 mL cold acetic anhydride was added over a period of 5 min. Sulfuric acid (98%) of 0.38 mL as the catalyst was diluted with 10.0 mL glacial acetic acid and was added to the reaction system over a period of 10 min. The temperature was controlled at 70 °C, and then held at this temperature for 20, 90, 120, 150 and 180 min to prepare yellow ginger starch acetates with DS of 0.09, 0.50, 1.51, 2.26 and 2.67, respectively. When the reaction was completed, the hot starch acetate solution was added to distilled water to terminate the reaction. The ratio of reaction solution to water was maintained at about 1:10. The precipitated product was collected on a Buchner funnel, washed by distilled water until neutrality, transferred to a glass jar and dried at 50 °C in a vacuum oven overnight [14].

2.4. The determination of the degree of the substitution

Determination of DS by titration involved complete basic hydrolysis of the ester linkages and titration of the excess alkali [15]. The starch acetate grounded sample of 0.5 g was accurately weighted and dissolved with acetone (25 mL), then an exact amount of aqueous solution of sodium hydroxide (0.50 M, 25 mL) was added and the solution was stirred for 1 h at room temperature. After indicator (phenolphthalein) was added, the excess of alkali was titrated with 0.50 M hydrochloride acid. The reference sample and duplicate sample were treated in a similar way.

The acetyl content (*A*%) was calculated according to following equation [15]:

$$A\% = \frac{(V_0 - V_n) \times N \times 43 \times 10^{-3}}{M} \times 100\% \quad (1)$$

where V_0 (mL) is the volume of 0.5 M HCl used to titrate the blank, V_n (mL) is the volume of 0.5 M HCl used to titrate the sample, N is the concentration of the HCl (M) used, M (g) is the amount of dry starch acetate sample, number 43 is the formular weight of acetyl groups. The acetyl content (*A*%) was used to calculate the degree of substitution, DS, according to the following equation [15]:

$$\mathrm{DS} = \frac{162 \times A}{43 \times 100 - (43 - 1) \times A} \quad (2)$$

where 162 is the molecular weight of anhydroglucose unit, 43 is the formular weight of acetyl groups, and 1 is the atomic mass of hydrogen.

2.5. Fourier transform infrared (FT-IR) spectroscopy

The FT-IR spectra of the native starch and starch acetates were recorded with an IR spectrometer (Bruker Vector 22), using potassium bromide (KBr) discs prepared from powdered samples mixed with dry KBr in the ratio of 1:30.

2.6. Scanning electron microscopy (SEM)

The morphological features of the native starch and starch acetates of different DS were observed with a scanning electron microscope (ESEM Philips XL-30). The dried samples were mounted on a metal stub and sputtered with gold in order to make the sample conductive, and the images were taken at an accelerating voltage of 20 kV. Micrographs were recorded at 500× magnification to assure clear images.

2.7. X-ray diffraction

X-ray diffraction patterns of the native yellow ginger starch and starch acetate were analyzed using Rigaku D/max 2500 X-ray powder diffractometer (Rigaku, Tokyo, Japan) with nickel filtered Cu Kα radiation (λ = 1.54056 Å) at a voltage of 40 kV and a current of 200 mA. The scattered radiation was detected in the angular range of 5–60° (2θ), with a scanning speed of 8° (2θ)/min and a step of 0.06° (2θ).

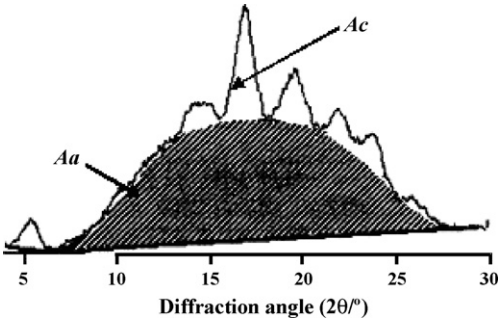

Fig. 1. Calculation of degree of crystallinity of the starches.

2.8. Determination of the degree of crystallinity

The degree of crystallinity of samples was quantitatively estimated, following the method of Nara and Komiy [16]. A smooth curve, which connected peak baselines, was computer-plotted on the diffractograms (Fig. 1). The area above the smooth curve was taken as the crystalline portion, and the lower area between smooth curve and the linear baseline which cover the 2θ range from 4° to 30° is taken as the amorphous section. The upper diffraction peak area and the total diffraction area over the diffraction angle 4–30° were integrated using the Smadchrom software (Morgan and Kennedy Research, Australia). The ratio of upper area to total diffraction is used as the degree of crystallinity. The equation for calculating the degree of crystallinity is as follows:

$$X_c = \frac{A_c}{A_c + A_a} \quad (3)$$

where X_c refers to the degree of crystallinity, A_c refers to the crystallized area on the X-ray diffractogram, and A_a refers to the amorphous area on the X-ray diffractogram.

2.9. Thermogravimetry analysis (TGA) and differential thermal analysis (DTA)

The thermogravimetric measurements and differential thermal analysis were performed with a Pyris/Diamond TGA/DTA apparatus (PerkinElmer Co., America). Samples of about 10 mg were heated from 20 to 500 °C at a rate of 10 °C/min and a flow rate of 25 mL/min in a nitrogen atmosphere.

3. Results and discussion

3.1. XRD

X-ray diffraction measurements were performed to check if chemical modification altered the crystallinity of starch. The X-ray diffraction spectra of native starch and acetylated starches are presented in Fig. 2. The native yellow ginger starch had sharp diffraction peaks at 17.2° (2θ) and a few small peaks around 2θ of 15.1°, 18.4°, 23.4° and 26.5°, which indicated typical A-type pattern [12]. As can be seen in Fig. 2c, DS 0.50 acetylated starch showed a similar profile of native one, but it had a new peak at 9° (2θ), which appeared diffusion peaks of acetylated starch. However, DS 1.51 and DS 2.67 acetylated starch represented typical peaks of acetylated starches, which had wide peaks at 9° and 20° (2θ). X-ray diffraction results indicated that with esterification processing, crystalline structure of native starch was destroyed, the degrees of crystallinity decreased from 47.01% to 11.06% with increasing the DS. The intra- and inter-molecular hydrogen bonds were responsible for the highly ordered crystalline structure [17]. During esterification, acetyl groups replaced some of the hydroxyl groups on starch, reducing the formation of intermolecular hydrogen bonds and thereby resulting in the destruction of the ordered crystalline structure. As the DS of the starch acetate increased, there was an increased destruction or even loss of the ordered crystalline structure.

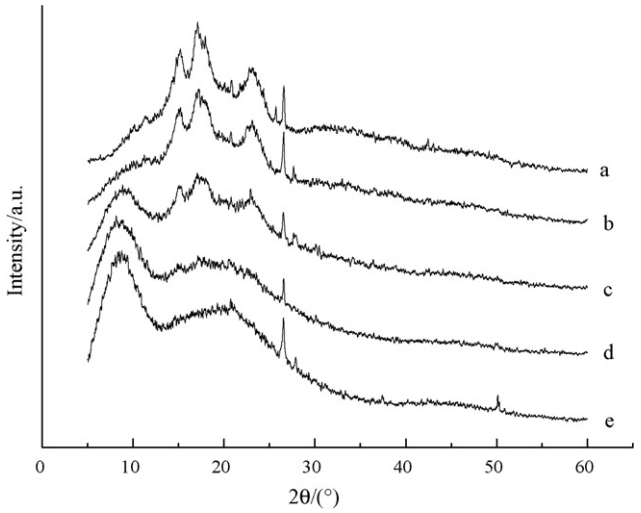

Fig. 2. XRD profiles of native starch (a) and acetylated starches at DS 0.09 (b), DS 0.50 (c), DS 1.51 (d), and DS 2.67 (e).

3.2. FT-IR

To detect the structure of acetylated starches, FT-IR spectra are recorded, and the spectra of the native starch, DS 0.09, 1.51, 2.67 acetylated starches are shown in Fig. 3. In the spectra of native starch Fig. 3a, there are several discernible absorbencies at 1159, 1082, and 1014 cm^{-1}, which were attributed to C–O bond stretching [18]. Additional characteristic absorption bands appeared at 992, 929, 861, 765, and 575 cm^{-1} are due to the entire anhydroglucose ring stretching vibrations. An extremely broad band due to hydrogen bonded hydroxyl groups appeared at 3421 cm^{-1} [19]. FT-IR spectra of different DS of acetylated starches showed some new absorption at 1750, 1435, 1735, and 1240 cm^{-1} assigned to carbonyl C=O, CH_3 antisymmetry deformation vibration, and CH_3 symmetry deformation vibration and carbonyl C–O stretch vibration, respectively. These new absorption suggest that the acetylated starch products were formed during esterification process. In addition, the broad band observed at 3100–3500 cm^{-1} for native starch,

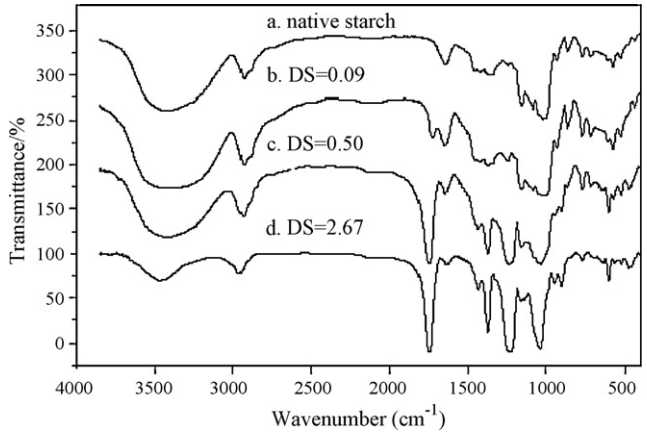

Fig. 3. FT-IR spectra of native starch (a) and acetylated starches at DS 0.09 (b), DS 0.50 (c), and DS 2.67 (d).

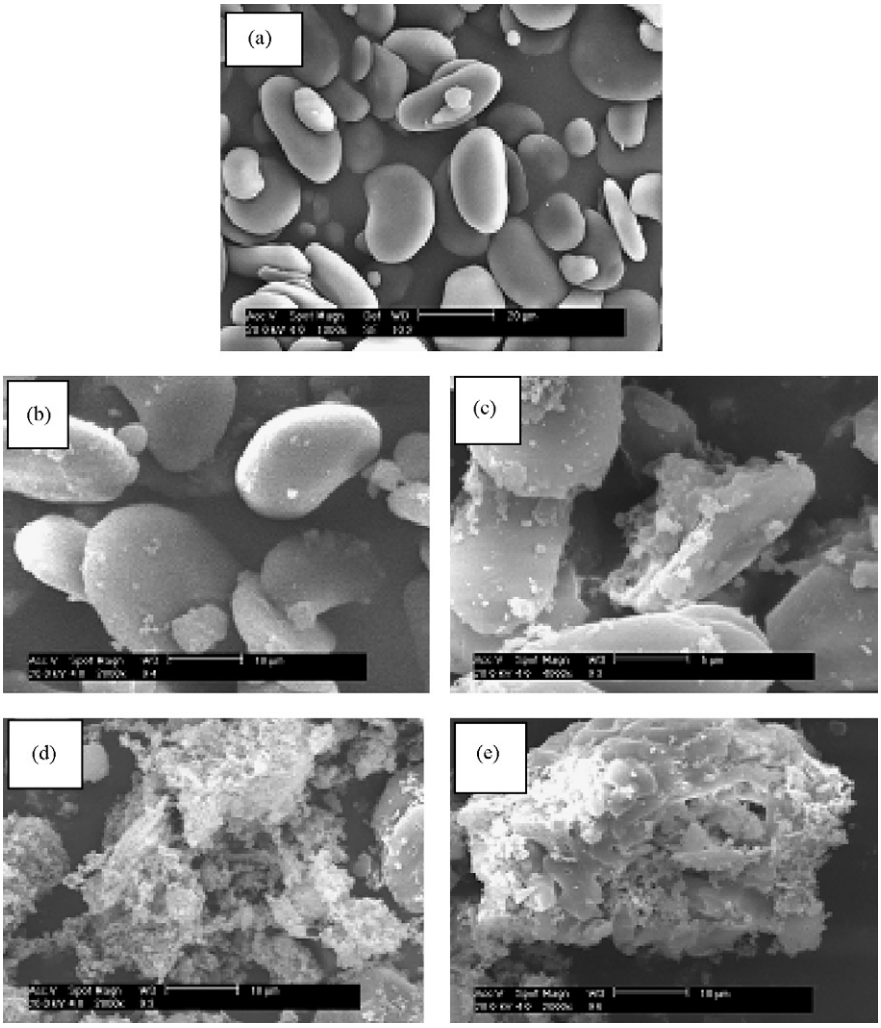

Fig. 4. SEM photographs of native starch (a) and acetylated starches at DS 0.09 (b), DS 0.50 (c), DS 1.51 (d), and DS 2.67 (e).

DS 0.09 and DS 1.51 acetylated starch clearly indicated the presence of free (absorption bands at 3400–3500 cm^{-1}) and bounded (shoulder at ca. 3250 cm^{-1}) hydroxyl groups. When DS reached to 2.67, the shoulder at ca. 3250 cm^{-1} disappeared, only a few free hydroxyl groups (absorption band close to 3500 cm^{-1}) still remained in the starch acetate. FT-IR spectroscopy showed that starch crystallinity is altered and this allowed the esterifying agents to have more access to the starch molecules for esterification processes. This observation also corroborates the X-ray diffraction results (observed in Fig. 2) that the ordered crystalline structure of native starch was destroyed and new crystal structure of acetylated starch was formed with increasing the DS.

3.3. SEM

Scanning electron microscopy was used to investigate the granule morphology of the native starch as well as the developments in esterification (Fig. 4). The results showed that the yellow ginger starch granules were oval to ellipsoid in shape with a few spherical ones, the starch granules lost their individuality and smoothness after esterification as a result of substitution of hydroxyl groups. As the DS of the starch acetates increased, there was an increasing destruction degree on the surface of the starch granules. As the starch acetates reached the higher degree of substitution, the starch almost fell into pieces, which revealed that the esterification not only happened on the surface but also in the inner structure of the starch. Once the reaction happened, the starch became looser and more porous, which accelerated the esterification to make the starch acetate granules become small fragments. This observation also corroborates previous investigations on corn starch [20] and yam starch [21].

3.4. TGA

The thermogravimetric curves were used to examine the changes in thermal stability caused by acetylation and to determine the weight loss of the material on heating. The TGA and DTG curves for the native starch and starch acetates were shown in Figs. 5 and 6, respectively. The native starch showed a two-stage weight loss below 500 °C, the first minor one corresponding to the loss of water around 60–100 °C and the other one corresponding to its decomposition. The derivatogram indicates that maximum decomposition occurred at the range of 277–353 °C. At 500 °C, 85.4% of the native starch was decomposed. As can be seen in Figs. 5b–e and 6b–e, acetylated starches also showed two-stage weight loss, the first weight loss that occurs between 200 and 320 °C is attributed to the decomposition of starch, followed by a decomposition of acetylated starch at the range of 330–420 °C. It was found that partially substituted samples (DS-values 0.09, 0.50, 1.51) have poor stability because their first region of weight loss occurred at lower temperature as compared to starch (Figs. 5 and 6). It is instructive that thermal stability of high DS acetylated starch is much better than

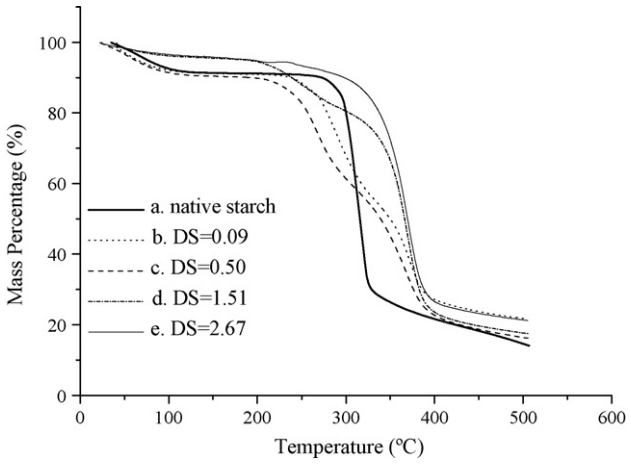

Fig. 5. TGA curves of native starch (a) and acetylated starches at DS 0.09 (b), DS 0.50 (c), DS 1.51 (d), and DS 2.67 (e).

that of the original starch when DS reached to 2.67, its intensity of the first weight loss almost disappeared. Thermal stability of starch acetates increases with increasing the degree of substitution. These results are in agreement with earlier studies concerning starch esters [22,23]. This increase in thermal stability with increasing DS was attributed to the low amount of remaining hydroxyl groups in starch molecules after acetylation. Since the main decomposition mechanism of starch is a result of the inter- or intra-molecular dehydration reactions of starch molecules with water as a main product of decomposition [24], the fewer the number of hydroxyl groups remaining, the better the thermal stability of the starch esters will be [25]. Therefore, a high DS had a beneficial effect on the thermal stability of the sample.

3.5. DTA

DTA was used to measure the occurrence of exothermal or endothermal changes with increase in temperature. The DTA curves of the native starch and the starch acetates were shown in Fig. 7. A broad endothermic peak appears in the DTA curve of native starch with a maximum at 314 °C, corresponding to the complete breakdown of starch. An endothermic peak was also observed in the curve of the low-substituted starch acetates (b), whose peak temperature (273 °C for DS 0.09 acetylated starch) was lower than that

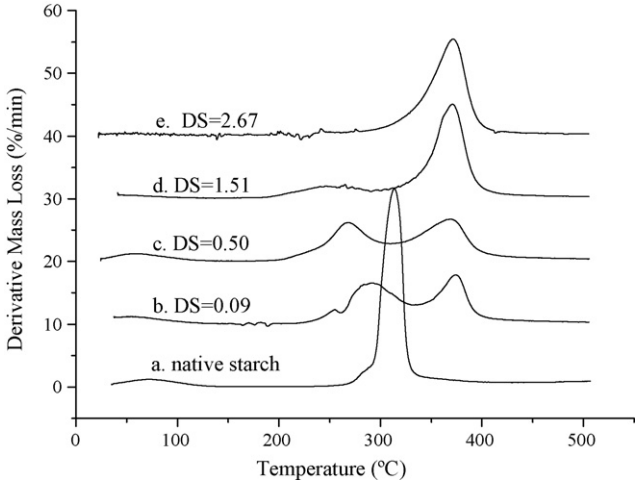

Fig. 6. DTG curves of native starch (a) and acetylated starches at DS 0.09 (b), DS 0.50 (c), DS 1.51 (d), and DS 2.67 (e).

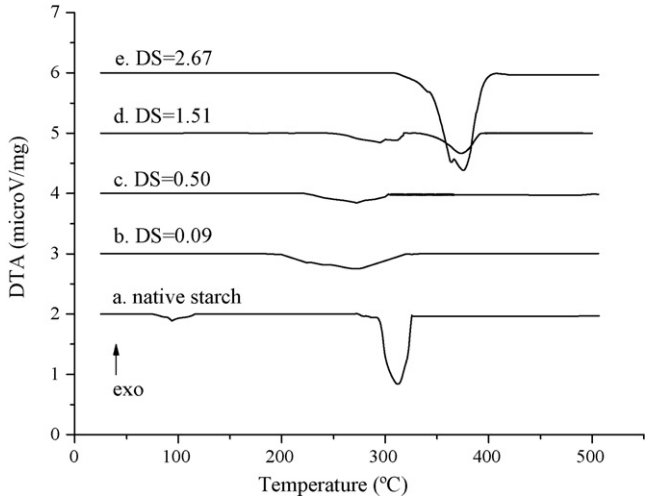

Fig. 7. DTA curves of native starch (a) and acetylated starches at DS 0.09 (b), DS 0.50 (c), DS 1.51 (d), and DS 2.67 (e).

of the native starch. There was a very weak endothermic peak in the curve of the low-substituted starch acetates (c). Such behavior might be expected because the crystal structure of part unmodified starch was disappeared and a new crystal structure of starch acetates was not formed (Fig. 2c). It was found that two endotherms emerges in the DTA cure of DS 1.51 acetylated starch, the first minor one are caused by the decomposition of starch, the other one are due to decomposition of substituted starch (peak temperature °C). In the case of DS 2.67 acetylated starch, an obvious endothermic peak occurs at higher temperature (peak temperature °C) as compared to starch (Fig. 7). It can be seen that thermal stability of high DS acetylated starch is much better than that of the original starch.

4. Conclusions

This study was carried out in order to understand and establish the changes in physicochemical properties of starch extracted from yellow ginger (*D. zingiberensis* C.H. Wright) after acetylation. Yellow ginger starch acetates with different degrees of substitution were prepared by reaction of native starch with acetic anhydride using sulfuric acid as catalyst. The DS values of starch acetates could be controlled by the acetylated addition such as temperature, reaction time, amount of acetic anhydride and so on. Structural modification of starch resulted in significant changes of the physicochemical properties of the starch. X-ray diffraction confirmed that the crystal structure of native starch was disappeared and new crystal structure of acetylated starch was formed at 9° and 20° (2θ). The FT-IR spectra revealed that the characteristic absorption intensities of esterified starch increase with the increasing DS. The SEM images showed a significant change in starch granule morphology, and most of the starch granules broke into pieces after esterfication. According to the experimental results of TG/DTG and DTA, the thermal stability of acetylated starch depends on the degree of substitution. Moreover, it was observed that the thermal stability of high DS acetylated starch is much better than that of the original starch when DS reached to 2.67.

Acknowledgements

This work was financially supported by the Applied Foundation & Leading Technology Research Program of Tianjin (Grant No. 08JCZDJC15300) and the National High-Tech Research and Development Plan of China (Grant numbers 2008AA10Z326). The authors

are grateful to Meng Ming, School of Chemical Engineering, Tianjin University, for their assistance with the TG/DTA measurements.

References

[1] X.L. Tang, Z.L. Xu, B. Xia, Med. Mater. 27 (2007) 877–880.
[2] X.Y. Wang, Z. Wang, D.L. Liu, Sci. Technol. 30 (2007) 94–97.
[3] F. Han, W.H. Li, D. Li, Chem. Ind. Eng. Prog. 26 (2007) 1501–1504.
[4] X. Sun, L.W. Deng, L.B. Wu, China Biogas 23 (2005) 25–28.
[5] M. Kaur, N. Singh, K.S. Sandhu, Food Chem. 85 (2004) 131–140.
[6] Y.X. Xua, Y.B. Dzenis, M.A. Hannaa, Ind. Crop. Prod. 21 (2005) 361–368.
[7] P. Taggart, in: A.C. Eliasson (Ed.), Starch in Food: Structure, Function and Application, Woodhead publishing Limited and CRC Press LLC, Cambridge/New York, 2004, pp. 363–392.
[8] O.S. Lawal, K.O. Adebowale, B.M. Ogunsanwo, Int. J. Biol. Macromol. 35 (2005) 71–79.
[9] A. Boutboul, P. Giampaoli, A. Feigenbaum, Carbohydr. Polym. 47 (2002) 73–82.
[10] M. Tarvainen, R. Sutinen, S. Peltonen, P. Tiihonen, P. Paronen, J. Pharm. Sci. 91 (2002) 282–289.
[11] Y. Yuan, L.M. Zhang, Y.J. Dai, J. Food Eng. 82 (2007) 436–442.
[12] Q. Zhou, W.J. Shi, L.Q. Zhang, Y.P. Li, X. Liu, J.Q. Kan, Food Sci. 28 (2007) 40–42.
[13] L.L. Wang, L.M. Zhang, Y. Yuan, W.Y. Gao, Nat. Prod. Res. Dev. 20 (2008) 52–54.
[14] L. Stefanos, F. Bernice, Chemometr. Intell. Lab. Syst. 36 (1997) 229–243.
[15] S.E. Rudoph, R.C. Glowaky, J. Polym. Sci. Polym. Chem. Ed. 16 (1978) 2129–2140.
[16] S. Nara, T. Komiy, Starch/Stärke 35 (1983) 407–410.
[17] Y. Xu, V. Miladinov, M.A. Hanna, Cereal Chem. 81 (2004) 735–740.
[18] S.M. Goheen, R.P. Wool, J. Appl. Polym. Sci. 42 (1991) 2691–2701.
[19] J.M. Fang, P.A. Fowler, C. Sayers, P.A. Williams, Carbohydr. Polym. 55 (2004) 283–289.
[20] J.F. Zhu, G.H. Zhang, J.G. Li, Chinese J. Appl. Chem. 23 (2006) 1010–1013.
[21] X. Wang, W.Y. Gao, L.M. Zhang, P.G. Xiao, L.P. Yao, Y. Liu, K.F. Li, W.G. Xie, Sci. China Ser. B: Chem. 51 (2008) 859–865.
[22] M. Elomaa, T. Asplund, P. Soininen, R. Laatikainen, S. Peltonen, S. Hyvarinen, A. Urtti, Carbohydr. Polym. 57 (2004) 261–267.
[23] E. Rudnik, G. Matuschek, N. Milanov, A. Kettrrup, J. Therm. Anal. Calorim. 85 (2006) 267–270.
[24] S. Thiebaud, J. Aburto, I. Alric, J. Appl. Polym. Sci. 65 (1997) 705–721.
[25] E. Rudnik, G. Matuschek, N. Milanov, Therm. Acta 427 (2005) 163–166.